5-2019

Active colloid behavior exhibiting soft-sphere characteristics for non-Newtonian solvent

Courtney Baier
University of Tennessee at Chattanooga, gnj279@mocs.utc.edu

Active colloid behavior exhibiting soft-sphere characteristics for non-Newtonian solvent

Courtney Baier

Departmental Honors Thesis

University of Tennessee at Chattanooga

Department of Chemistry and Physics

Examination Date: 27 March 2019

Dr. Luis Sanchez-Diaz
Professor of Physics
Project Director

Dr. Joshua Hamblen
Professor of Physics
Department Examiner

Abstract

The purpose of analyzing soft-sphere Brownian particles with varying velocities and densities is to be able to predict their interaction behavior once a force has been applied. The particles portray different behaviors depending on if the particles are passive or active Brownian particles. The data studied was collected from simulations, and there are no attractive forces involved in the particles' interactions. Mean square displacement graphs, radial distribution graphs, structure factor graphs, and viscosity as a function of density and velocity were used to examine and compare the data generated. Experimental data was analyzed by a program to be interpreted into a mean square displacement graph. It has been determined that once particles form into clusters, the clusters do not remain static, but they interact as a dynamic system. For the analysis of viscosity, it has been determined that an increase in density always results in shear thickening. However, an increase in velocity creates an overall shear thickening trend, but an increased velocity of the particles results in clusters splitting into two small clusters leading to a shear thinning effect. These results allow for a better understanding of Brownian particle behavior given different environmental factors such as magnitude of force.

Table of Contents

Chapter 1: Introduction

1.1 Purpose of Current Research

To expand on the previous research on active colloid simulations, the current research goes further in-depth on the hard-sphere model to describe particle interactions when the particles behave as passive Brownian particles and active Brownian particles. With mean square displacement (MSD) describing the travel distance of each step, and radial distribution function [g(r)] and structure factor [s(q)] describing the phase structure of the suspensions, these forms of analysis are used to compare the different densities and particle velocities of colloidal systems. The analysis of Newtonian fluids becoming complex fluids was also assessed through simulations to determine how the behavior of active Brownian particles from a solute affects the behavior of passive Brownian particles in a solvent.

1.2 Brownian Motion

Brownian Motion is the random motion of particles in the form of passive motion or active motion. The particles that possess passive motion are in a state of equilibrium for thermal energy. Active Brownian particles display out of equilibrium characteristics in which their thermal energy changes or they propel themselves out of equilibrium.[1] Even though passive Brownian particles do not display self-propulsion, their random movement is caused by collision with surrounding fluid molecules resulting in the fluctuation of their thermal energy. The passive Brownian particles can be used to essentially "zero-out" a system for noise in order to determine the true potential energy of active particles in a system. Passive Brownian motion can be described as the translational diffusion coefficient, D_T, and can be applied in the equation (1) in which k_B is the Boltzmann constant, T is the temperature, η is the viscosity, and R is the radius of the particle.[2]

$$(1) \qquad D_T = \frac{k_B T}{6\pi\eta R}$$

Equation (2) also plays into active Brownian motion in which it calculates the rotational diffusion coefficient, D_R. D_R is dependent upon the volume of the particle, R^3.

$$(2) \qquad D_R = \frac{k_B T}{8\pi\eta R^3}$$

Active Brownian particles still exhibit random motion in which their projected angle is changed from colliding into surrounding particles. The only difference is that the potential energy is greater in an active particle because it is not strictly dependent upon thermal energy fluctuations.

The thermodynamic ensemble use was the canonical ensemble (NVT). The closed system is held at constant volume and constant temperature which is room temperature (28 °C). The particles come into weak thermal contact with particles of the same temperature.

1.3 Active Colloids

Active colloids consist of active particles suspended in a passive diffusion fluid. In computational studies, the noise is able to be subtracted out of a potential energy calculation by determining the potential energy of the solvent. The solvent only interacts with the active particles as hydrodynamic friction and to transfer momentum.[2] The force generated for active colloids stems from energy that the particles consume to generate their own energy gradient rather than relying on an external energy gradient such as gravity or surface forces to diffuse through. Because the active particles generate their own gradient, they are able to change their direction of propulsion when a change in thermal noise is experienced.[3]

It has been observed that cells such as *Escherichia coli* and algae display active Brownian behavior like chemotaxis and gravitaxis. Recently, the topic of interest is to apply the knowledge

of active Brownian motion to artificial particles for transportation at the microscale size.[4] In perspective of studying the changing viscosity of non-Newtonian fluids, interest has arose to study how non-Newtonian fluids affect the Brownian behavior of particles.[5]

With being able to predict the behavior of Brownian particles, these particles can be controlled and used for a variety of applications such as micro-transporters in which they can carry cargo to transport a molecule in the body or a cell. For the material science aspect, these particles can be woven into clothing to act as a protective barrier when it shear thickens under a high enough shear stress.

1.4 Shear Thickening and Shear Thinning

Shear thickening and shear thinning is the result of a viscosity change when a shear stress (or a pressure in the x-direction) is applied resulting in the particles in the system to rearrange in a certain way. The way the particles arrange themselves is due to how the particles interact with each other. So some systems do not experience any viscosity changes under shear stress, so the particles interact with each other the same way as if there is no shear stress applied. For systems that experience shear thickening, particles will cluster together to where several clusters exist with just a few loose particles traveling in between them. Shear thinning systems display the particles forming into layers which allow the particle layers to easily slide off each other. At low shear stress, shear thinning occurs. However, when a sudden onset of high shear stress occurs, shear thickening is displayed in the system. It has been found that through experiments, shear thinning is displayed no matter how high the shear stress when the density of the system is low. The only time shear thinning transitions to shear thickening is when the density reaches a critical point to allow for the particles to interact with each other.[6]

1.5 Viscosity

It has been observed that the behavior of active particles changes depending on if they are suspended in a Newtonian fluid or a complex fluid. The added stress that is applied to a complex fluid by the active particles' gradient restricts the Brownian motion. Another observation has yielded results that suggest that active colloid particles can cause the Newtonian fluid to gain complex fluid characteristics. The cause of sheer thickening is the extra pressure applied resulting in the particles to interact more with each other.[5] The diffusion coefficient for an isolated spherical Brownian particle, D_0, is inversely proportional to the pure solvent viscosity, η_0.[7] The hydrodynamic interactions from the boundary surfaces plays a role in the dynamics of viscosity as when hydrodynamic forces are present, the majority of particle interactions are hosted at the walls.[8]

1.6 Phase Separation from Clustering

When a colloid is experiencing active Brownian motion, the non-zero velocity allows the particles to cluster together even though there are no attractive forces present. With low densities, a single cluster forms. When the cluster reaches a certain size, it splits apart into two smaller clusters. Cluster formation is negligible of the velocity of the particles. The only restriction on velocity is that the particles cannot be diffusive. Phase separation occurs only in higher densities when enough large clusters form to the point where the density for the surrounding particles is extremely low (no interaction) causing a gas phase.[9]

Chapter 2: Methods and Materials

2.1 Introduction to Experimental Simulations

This research focuses on the movement of particles in a colloidal suspension. The active particles which have self-propelled movement are out of equilibrium and are compared to passive colloid particles which have a velocity of 0 $\mu m*s^{-1}$ are in equilibrium. The program is ran on python code. Initially, the active colloid program is studied by just analyzing one particle in a system. The experiment is held at constant volume and temperature, and the mean squared displacement is analyzed to observed through time how much space is covered through free range movement. The program is later progressed to two and more particles to observe how system particle density affects the mean squared displacement. A force function is written to follow the hard-sphere model so that particles cannot overlap each other thus not allowing for kinetic energy to be absorbed by the impacted particle.

2.2 Force Program

The interaction between the simulated binary colloidal particles is described by the pairwise repulsive soft sphere potential. Mathematically, this may be written in equation (1) where σ is the diameter of the particles, and ε the interaction strength.

$$(1)\ V(r) = 4\varepsilon\left[\left(\frac{\sigma}{r}\right)^{12}\right]$$

The force is calculated by determining the virial function w, equation (2). Because the repulsive forces displayed in Figure 2.2.1 are dependent upon the exponential value in equation (1), the exponential value can vary depending upon the desired magnitude of the repulsive forces. In this case, the repulsive force increased in order to have the particles display the hard-sphere model but without the attractive forces present. So equation (1) is derived to form the new force equation for it to be substituted into equation (2) for the virial function.

$$(2)\ w = \frac{r}{3} * F$$

$$F = 48\varepsilon\left(\frac{1}{r}\right)^{14}$$

$$w = \frac{r}{3} * 48\varepsilon\left(\frac{1}{r}\right)^{14} = \frac{48}{3} * \varepsilon\left(\frac{1}{r}\right)^{13}$$

Figure 2.2.1 Soft-Sphere potential energy graph[10]

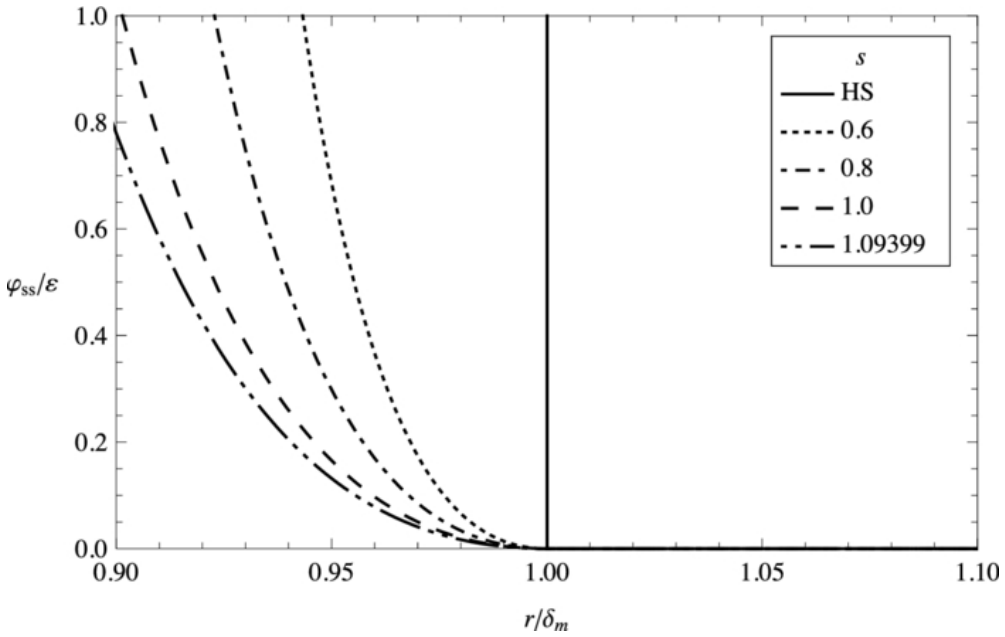

The force program allows the particles to slide off each other and to not automatically stick to each other upon contact. The force program was ran on Python with NS = 5,000,000 steps at densities ρ = 0.3 and 0.6 with velocities v = 0, 3, 7, and 30 μm$*$s^{-1} for 800 particles. These were qualitatively analyzed through VMD[11]. VMD is a computational software that forms an image of the behavior of the particles that were written. The results from the variation of different densities were assessed through graphs of g(r) as a function of r and MSD as a function of time (s).

2.3 Coordinates

2D Brownian dynamic simulations of an active colloid suspension were performed. The algorithm used in this work was proposed by Ermak and McCammon[10], without hydrodynamic interactions and with an additional term to simulate the propulsion velocity found in the experimental active colloids. The resulting equation can be written in the following way to generate the new position, $x(t + \Delta t)$ and $y(t + \Delta t)$, from the current position, $x_i(t) and\ \ y_i(t)$.

The main program is written to incorporate the force program that was defined in the section before. The equations below give rise to the coordinates of particles. The MSD graphs follow these equations by measuring the distance traveled through each timestep taken by the coordinates. Equation (3) calculates the angle at which the particle is projected. Equation (3) is essential as it determines with other particles' angle projections how many particles will be in a cluster and where the particles will transfer. Equations (4) and (5) respectively calculate the x and y coordinates using the calculated angle from equation (3).

$$(3)\ \varphi_i = \varphi_{i-1} + \Omega * \Delta t + \sqrt{2 * DR * \Delta t} * w_{\varphi,i}$$

$$(4)\ x_i = x_{i-1}(t_0) + v * cos\varphi_{i-1} * \Delta t + \frac{F_x D}{k_B T} * dt + \eta_i(t)$$

$$(5)\ y_i = y_{i-1}(t_0) + v * sin\varphi_{i-1} * \Delta t + \frac{F_y D}{k_B T} * dt + \eta_i(t)$$

With φ_i meaning particle orientation, Ω as angular velocity, Δt as the time step, DR is rotational diffusion, $w_{\varphi,i}$ is independent white noise, $F_{x,y}D$ is the force in the x and y direction, T is temperature, dt is time, and η_i is noise.

The initial configurations were generated using the following procedure: first, particles were placed randomly in the simulation box at the desired density, and then the overlap between the particles were reduced or eliminated. Once the initial configuration was constructed, several

thousand cycles were performed to lead the systems to equilibrium, followed by at least two million cycles where the data was collected. It was observed that whether using 1,500 particles or 4,000 particles, the results are similar. There is no systematic effect of system size in the calculation of these properties.

2.4 Pressure

The particle in a box theory is applied to analyze the pressure created by the force of the particles colliding into the walls of the 2-dimensional box. The size of the box, area, is determined by equation (6) which is dependent upon the number of particles and the density desired for analysis.

$$(6)\ area = \sqrt{\frac{NP}{\rho}}$$

The value of the area of the box is used in equations (7) and (8). These equations use the coordinates generated by equations (4) and (5) as initial coordinates in each step which are to be combined with the area of the box to create new coordinates.

$$(7)\ x = x_i + area * \left(\frac{x}{area}\right)$$

$$(8)\ y = y_i + area * \left(\frac{y}{area}\right)$$

The virial function (w) is used in combination with $V(r)$ and the number of particles (NP) to generate a new w after each step in equation (9).

$$(9)\ w = w_i + \frac{V(r)}{NP}$$

w is used in a similar manner to calculate the pressure, P, generated by each particle after each step in equation (10)[12]. N is the number of steps in the simulation, k_B is the Boltzmann constant, T is temperature in Kelvin, and A is the area of the box.

$$P = \frac{Nk_BT + \langle w \rangle}{A} \quad (10)$$

2.5 Mean Square Displacement

Mean Square Displacement (MSD) is generated by means of writing the distance a particle travelled in a time step as the function of time in seconds. Time is calculated in equation (11) where dt is the time step at which a measurement was taken.

$$time = (NFrec) * (\mathrm{d}t) \quad (11)$$

NFrec is the frequency at which the particles were measured in each time step, and dt is the time. MSD is expressed as wx and wy for the x and y coordinates, respectively. The initial and final coordinates after each step are determined from the pressure program. wx and wy are calculated through equations (12) and (13), respectively.

$$wx = wx_i + (x - x_i)^2 \quad (12)$$

$$wy = wy_i + (y - y_i)^2 \quad (13)$$

wx and wy are combined to form the total MSD, wt, in equation (14) where NTMax is the number of configurations saved.

$$wt = \frac{1}{4} * \frac{wx + wy}{(NTMax * NP)} \quad (14)$$

2.6 Radial Distribution Function

The radial distribution function, g(r), is a histogram of the probability of the number of particles being distance r from one another. This can only be applied to a suspension that contains only 1 type of particle. The units used is σ which 1 σ is the distance between the center of particle 1 to the center of particle 2 when they are in direct contact with each other. The area of the box is dependent upon the density with the number of particles remaining constant. So as

the density increases, the size of the box decreases. Equation (15)[13] determines the number of particles within distance r of each other. When analyzing the graphs, the primary distance of interest is 1 σ because it will best explain what densities or velocities result in particles merging the closest.

$$(15) \qquad g(r) = \frac{A}{NP^2}\langle \sum_i \sum_{j \neq i} (r - r_{ij}) \rangle$$

2.7 Structure Factor

Structure factor [S(q)] is a Fourier transformation that explains the density changes in a suspension. It is closely related to g(r) which is observed in equation (15)[12]. The integration of g(r) allows for the determination of the density in a sample. The program uses equation (16) to predict the intensity of light scattering [S(q)] if quantity (q) of light is applied to the sample. ρ is the density of the suspension.

$$(16) \qquad S(\mathrm{q}) = 1 + 4\pi\rho \int_0^\infty [g(r)] \frac{\sin qr}{qr} r^2 dr$$

2.8 Viscosity

The pressure of the system that is caused by the particles colliding is used to determine the viscosity of the colloidal suspension. The viscosity is written in the force program as equation (17)[14]for 100 particles. Equation (17) will generate the average viscosity of all particles in each step, N. The data is saved in a file to be analyzed to determine the overall viscosity of the colloidal sample. The viscosity data is analyzed for each step to determine the average viscosity. $\sigma(i)$ is the initial pressure and $\sigma(i + j)$ is the final pressure in that step. σ is the pressure from shear stress in the x-direction and force in the y-direction. Pressure is integrated to cause the

particles to collide with respect to time. dt is the time step multiplied by the frequency of data collection (NFrec = 300). The program ran on N = 26,167 arrays.

$$(17) \qquad viscosity = \frac{A}{k_B * T} \int \langle \sigma(i+j) * \sigma(i) \rangle dt$$

2.9 Experimental MSD

The viscosity was experimentally determined through the use of a program written to track the x and y coordinates of particles that were analyzed through a camera hitched to a compound microscope. The microscope used was an AmScope T690C microscope (S/N: 1754634) with a 40X objective lens and 10X ocular lens. The camera that was used is an AmScope MU1400 microscope digital camera (S/N: 1605190367). The program that was used to analyze the system is Imagej. Equation (19)[15] was used to calculate the MSD which uses equation (18)[15] to calculate the average.

$$(18) \qquad r^2 = (x - x_0)^2 - (y - y_0)^2$$

$$(19) \qquad \langle r^2 \rangle = \frac{\left(\sum_{n=1}^{N} r_n^2\right)}{N}$$

N is the number of steps which was set to 8,000,000 steps, and n is the time in-between each frame. n = 0.00001 for densities < 0.7. Densities > 0.7 require for n to be equal to 0.000001 or less or else the program loses track of the particles and is not able to calculate the MSD or any other data points. The particles that were analyzed were 2.0 μm microspheres. The category number is Cat# 19405, and they are a Polybead®Sulfate beads. The concentrated suspension is 3% solute and 97% solvent with the solvent being deionized water (dH_2O). The three dilutions that were analyzed were 1 drop:100 mL dH_2O, 2 drops:100 mL dH_2O, and 4 drops:100 mL dH_2O. The pipette used to transfer the diluted solution to a microscope slide is a Fisherbrand Finnpipette II 0.5 - 10 μL (S/N: GH89208). 5 μL of sample are transferred to a slide for analysis.

Two different types of slides were used to analyze the sample. A standard flat slide caused the sample to spread out farther when a cover slip was applied. A concave slide was used as well. The concave slide contained the sample better when the slide was applied. A cover slip is needed for analysis as it greatly limits noise from the environment such as air movement. When adjusting the microscope for analysis of the particles, it is essential to be as careful as possible to not cause vibrations to the sample as it results in noise and non-Brownian motion that the program will still analyze. The area that the samples remained in when not in use was kept at 4℃. It is also essential to work quickly, as the lamp in the microscope caused the sample to warm up faster than if it was simply exposed to a room temperature environment (28℃). The extra applied thermal heat also causes the water to evaporate at a quicker rate which results in a false density.

Chapter 3: Results and Discussion

3.1 Singular Particle

Figure 3.1.1 shows the simplified behavior of how the particles would behave if they did not interact with one another. It is seen that at velocity (v) = 0 $\mu m*s^{-1}$, the particle stays at a steady state of motion. The dynamic particles stay at a steady state, but later in time, the displacement begins to dip.

Figure 3.1.1 Single Particle Velocities 0-3 $\mu m*s^{-1}$

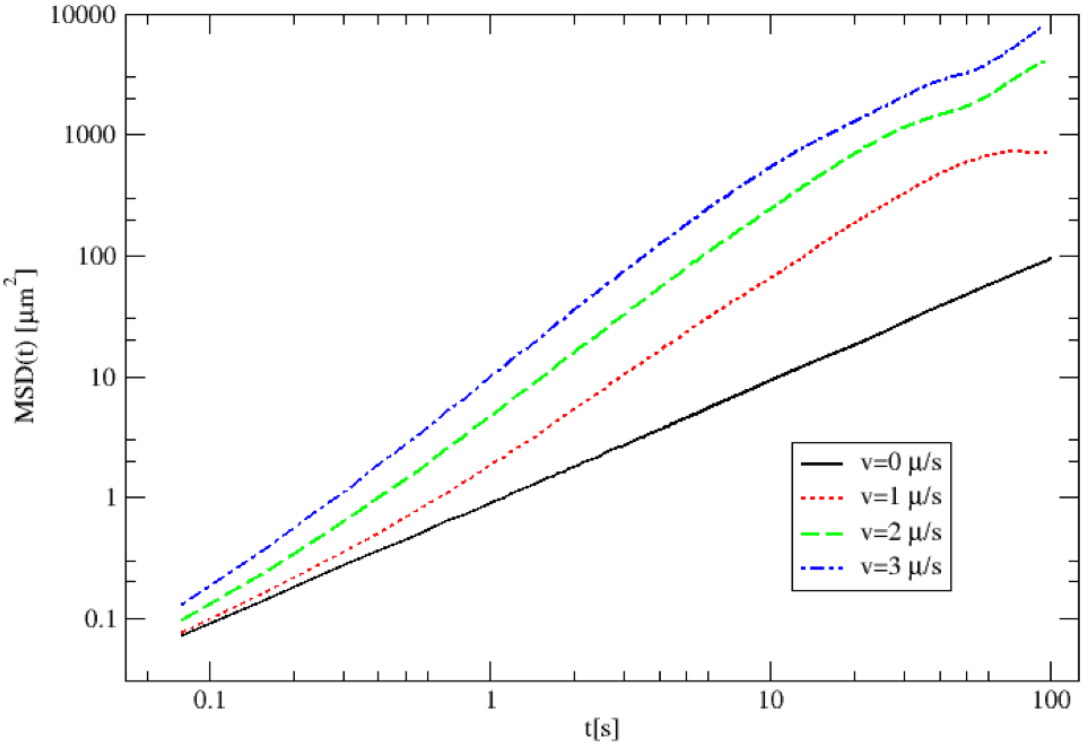

Behavior is as expected and opposite from collective motion solutions. The lowest velocity contains particles that stay closer together and do no move far, whereas the highest velocity contains particles that are more spread out and travel farther.

3.2 Statics and Dynamics Collective Motion (v = 0 μm$*$s^{-1})

With statics, there are varying densities, but the velocity is kept constant at 0 μm*s^{-1}. Because velocity is held constant, the particles are not clustering together. However, the particles just become closer together as the density increases. The density can be defined as $\rho = \frac{N\pi d^2}{4A}$ with N as the number of particles with a diameter of d in an area, A.

In Figure 3.2.1, the graph shows that the lower the density, the larger space the particles are covering due to the Brownian motion. Equations (3), (4), and (5) in section 2.3 are used to calculate the coordinates of each particle. This can be applied by measuring the distance in between each particle after each time step to measure the mean square displacement. ρ = 0.1 has a dramatically larger MSD than ρ = 0.2 because the area of the box decreases by half from 999.9 μm^2 for ρ = 0.1 to 499.9 μm^2 for ρ = 0.2. In a different application, the number of particles doubled going from ρ = 0.1 to ρ = 0.2. This results in the particles having a greater chance of colliding into each other thus resulting in a loss of distance travelled in each time step.

Figure 3.2.1 Mean Squared Displacement Densities ρ = 0.1-0.7

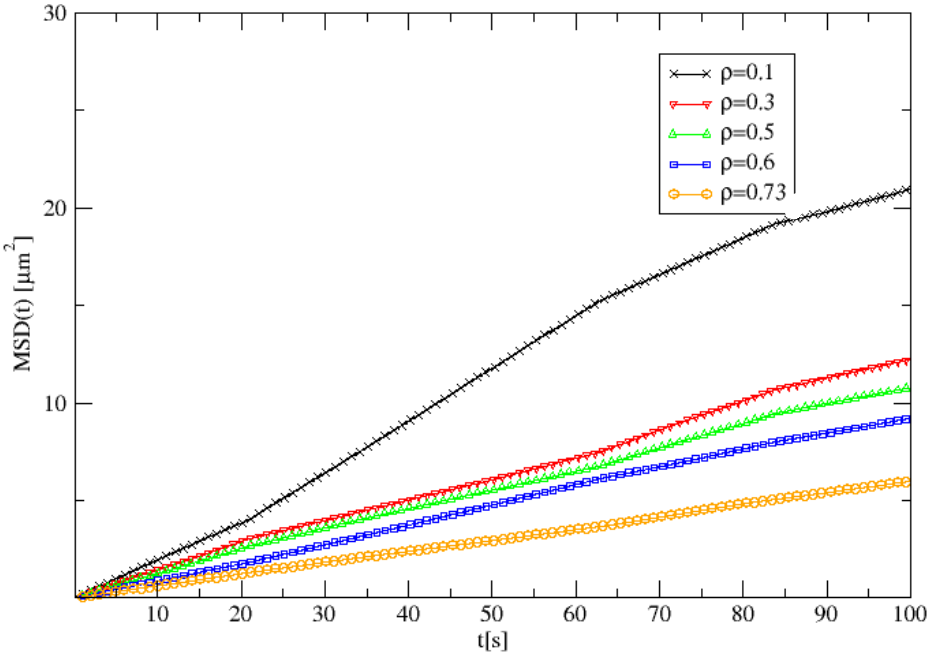

As mentioned for Figure 3.1.1, the results for collective motion are opposite for the distance travelled. In this instance, the varying densities are described. The lower densities do not interact with each other as much as the higher densities which allow for a higher distance travelled for lower density systems.

Figure 3.2.2 shows the radial distribution function is plotted as the number of particles, g, as a function of the radius of the particles, r, of ρ = 0.1-0.7. With velocity held at constant speed, the probability of particles touching each other increases as density increases. The x-axis, r, has the units of σ which means the distance between the center of two particles. So at 1.0 σ particles are touching but not overlapping due to repulsive forces observed by the hard sphere model.

Figure 3.2.2 Radial Distribution Function ρ = 0.1-0.7

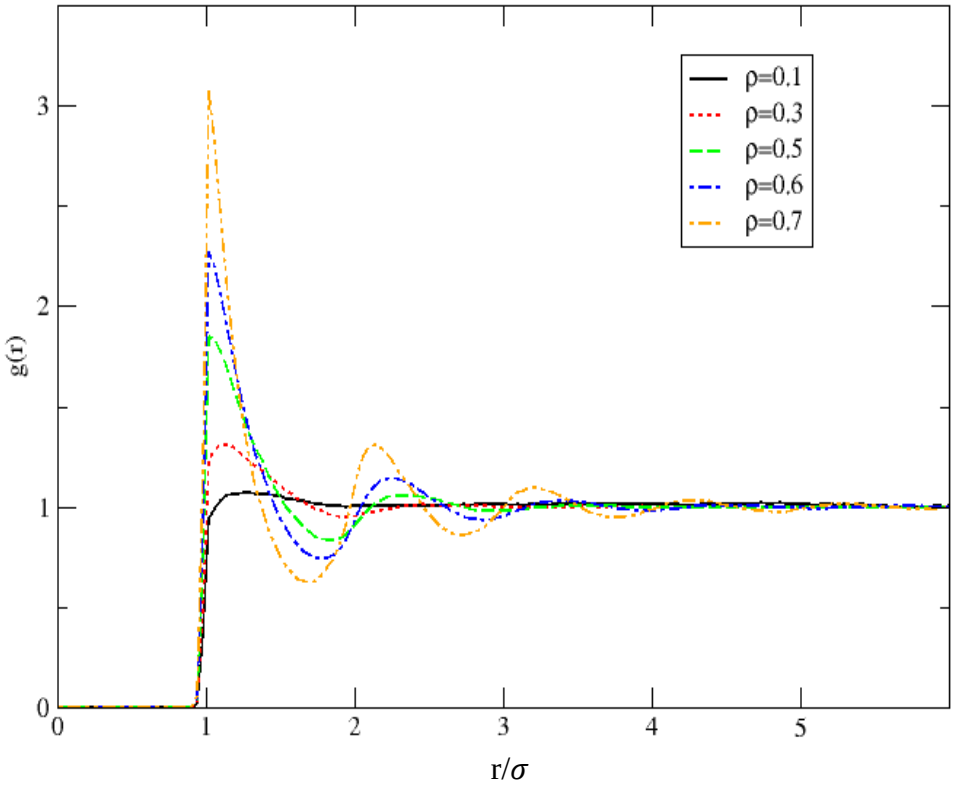

Velocity is zero, and the varying densities are behaving as expected with the highest one graphically displayed as a solid/dense fluid and the lowest one is displayed as a gas.

Figure 3.2.3 is the static structure factor that plots the scattering intensity, S(q), as a function of the scattering vector, q. Because the particles behave as a liquid, the graph does not depict sharp peaks, but the peaks do gradually increase in peak size as density increases which indicates that a more dense structure is formed. So the colloid suspension that has a ρ = 0.7 produces more intense scattering characteristics than the lower densities when q = 6 σ. With a high intensity of scattering, this indicates a cluster has been formed for the suspension of ρ = 0.7.

Figure 3.2.3 Structure Factor for ρ = 0.3-0.7

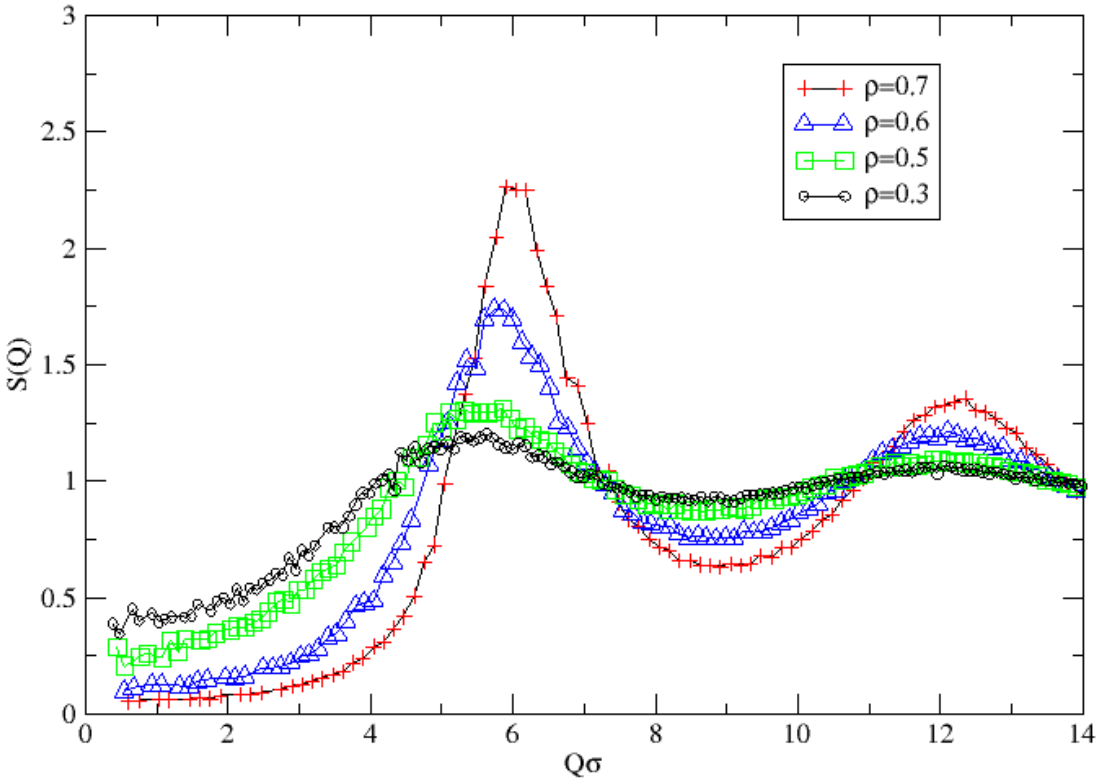

With velocity set to 0 μm*s^{-1}, the intensity of the scattering light (Q) has to be relatively high (6 σ). With the particles being passive Brownian particles, the low-density colloids have a lower probability of interacting with each other as opposed to the high-density colloids.

Figure 3.2.4 shows the relationship of the suspension with a ρ = 0.3 and a constant velocity of 0 with 800 particles. With the empty pockets that are scattered, the particles are able to travel farther as a colloidal suspension with a lower density as compared to Figure 3.2.5 which was predicted by Figure 3.2.1. Figure 3.2.2 accurately predicts the number of particles that surround each other as a colloidal suspension with a lower density compared to Figure 3.2.5. This figure displays how the lower densities are not able to scatter light as well as colloidal suspensions with a higher density (Figure 3.2.5) which is explained by Figure 3.2.3.

Figure 3.2.4 ρ = 0.3 Velocity 0 μm*s^{-1}

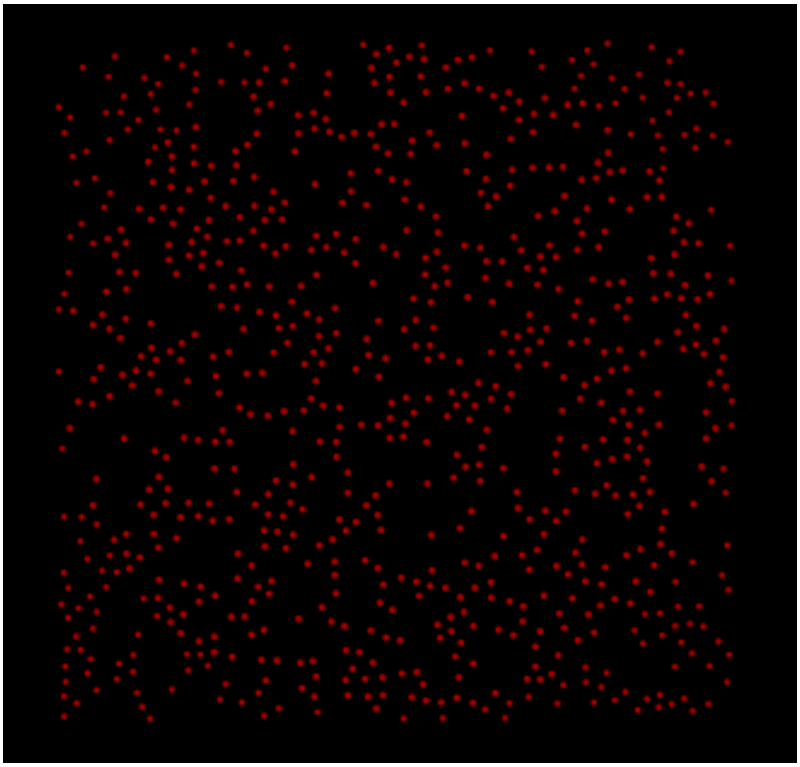

Figure 3.2.5 can be compared to Figure 3.2.4 in that the velocity is held constant at 0 μm*s^{-1} and it also portrays the hard sphere model, but it has a higher density at ρ = 0.6. This figure demonstrates the results given by Figures 3.2.1, 3.2.2, and 3.2.3. Because the velocity is 0 μm*s^{-1}, the particles are passive and not active, so the colloids are not able to cluster. However, they do merge closer together as the density increases which is explained by Figure 3.2.1. With the particles not as spread out as the colloidal suspension of ρ = 0.3, this figure displays the results of Figure 3.2.2 in that there are more particles within a certain radius of σ around one another. Even though there is no clustering portrayed in this figure, it still defends the data generated by Figure 3.2.3 in that this colloidal suspension has a higher intensity in the ability to scatter light than the colloidal suspension represented by Figure 3.2.4.

Figure 3.2.5 ρ = 0.6 Velocity 0 μm*s^{-1}

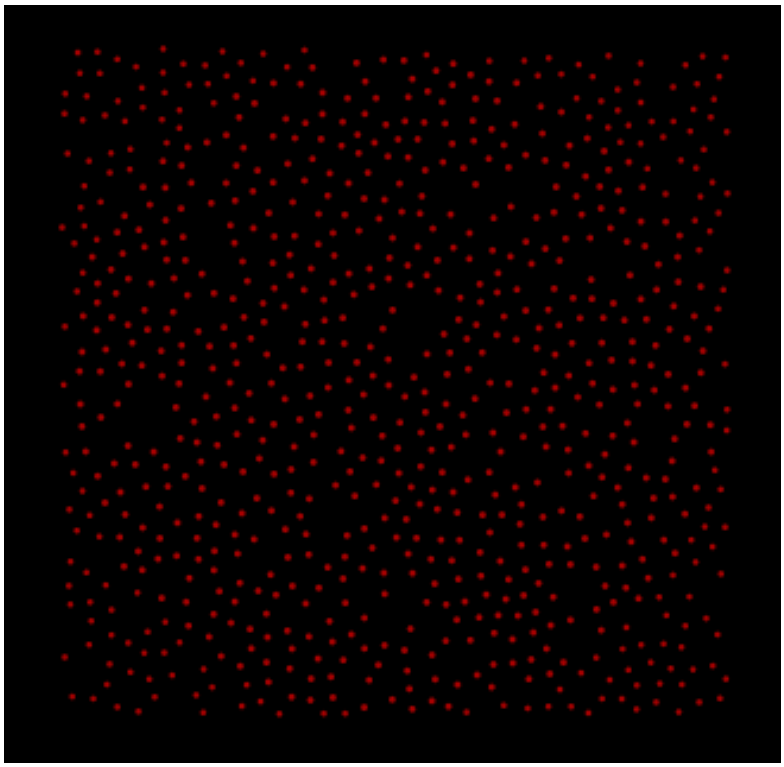

3.3 Statics and Dynamics Collective Motion (v > 0 μm*s^{-1})

In nonequilibrium driven systems, entropy decreases when active particles become agitated. The agitation is caused by a force that results in the active particles propelling themselves. The particles will then act like they are in a freezing process by forming a large dense cluster with a dilute gas phase surrounding. This displays a non-Newtonian characteristic.[9]

Figure 3.3.1 shows the mean square displacement of a system with a density of 0.3 and varying velocities in the range of 0-5 μm*s^{-1}. It is seen that each interval of velocity doubles in distance travelled as velocity increases.

Figure 3.3.1 Mean Square Displacement Velocities 0-5 μm*s^{-1} ρ = 0.3

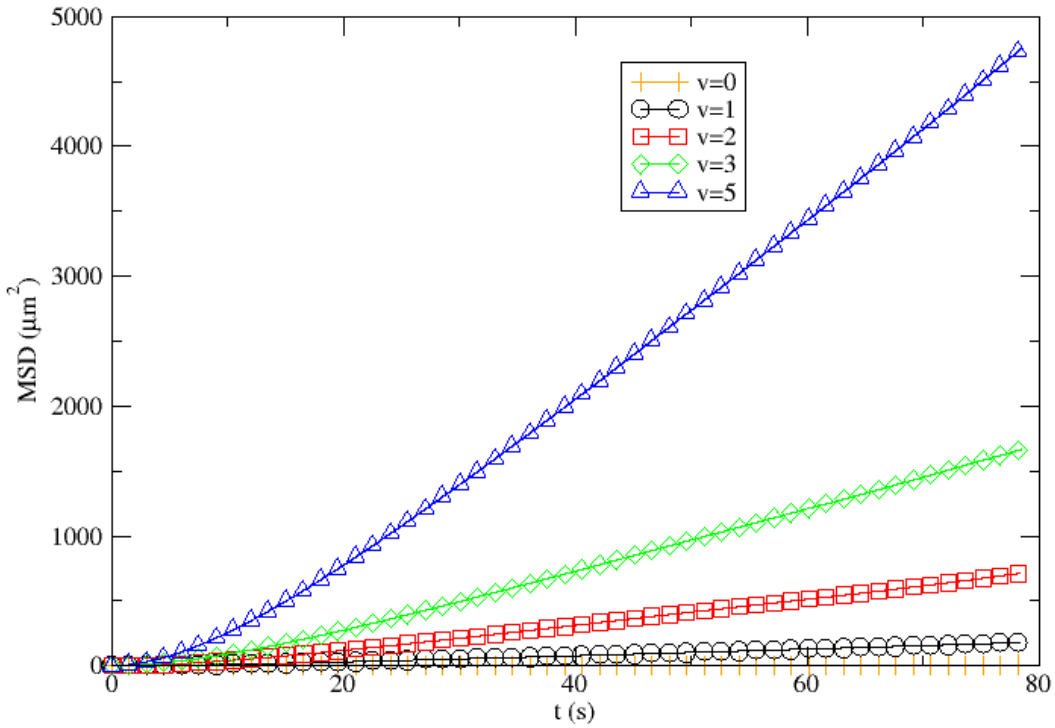

The results are as expected for a dynamic collective motion system. With density remaining stagnant, this shows that the concentration of particles affects the amount of hydrodynamic forces that are exposed to the travelling particles resulting in the travel pattern to be altered.

Figure 3.3.2 shows the number of particles surrounding each other with varying velocities held at a constant ρ = 0.3. It demonstrates that as velocity increases, the number of particles at 1 σ increases. In this figure as compared to Figure 3.2.2, the number of particles around a single particle increases from about 1.5 to 5 for the velocity of 0 μm*s^{-1} and a ρ = 0.3 at 1 σ.

Figure 3.3.2 Radial Distribution Function Velocities 0-7 μm*s^{-1} ρ = 0.3

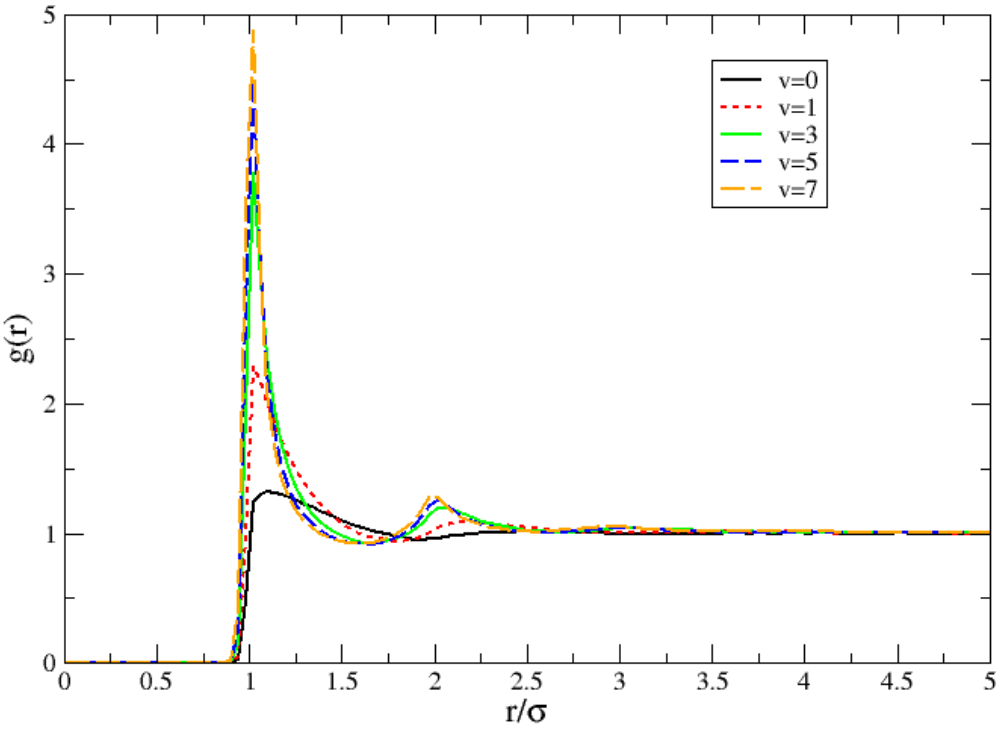

Active Brownian particles at a low density display increasing interaction as the velocity increases. The sharp peak for velocity 7 μm*s^{-1} indicates that the particles are colliding into each other resulting in the formation of clusters. The dramatic increase in peak height from velocity 1 μm*s^{-1} to velocity 3 μm*s^{-1} is the result of particles with a low velocity forming clusters, but the increased time for particles to find each other results in clusters being given the chance to separate into two different clusters which results in a lower probability of particles surrounding each other.

Figure 3.3.3 shows the structure factor for a colloidal suspension with varying velocities and a ρ = 0.3. It can be compared to Figure 3.2.3 for the plot demonstrated by ρ = 0.3. It is seen that density has more weight for the determination of the intensity of light scattered with the max S(q) at about 2 σ for velocity 7 μm*s^{-1} in Figure 3.3.3 and 2.25 σ for ρ = 7 in Figure 3.2.3. However, due to the particles in a dynamic suspension, the intensity of S(q) has been detected at a scattering vector of near 0 σ rather than 6 σ.

Figure 3.3.3 Dynamic Structure Factor Velocity 0-7 μm*s^{-1} ρ = 0.3

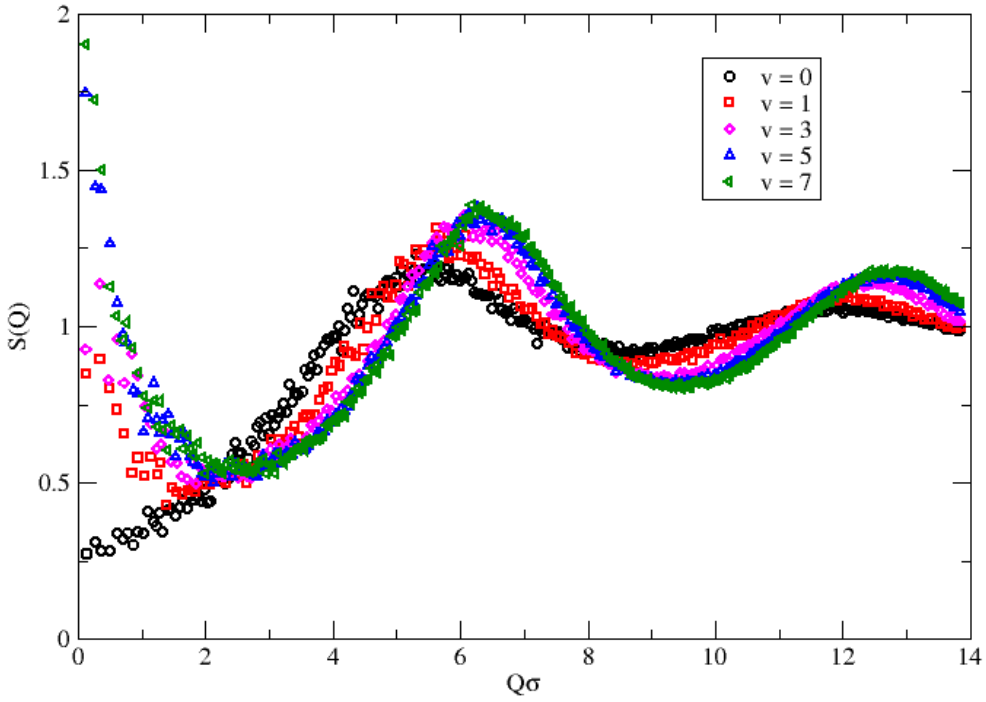

This increase of S(q) detected at low q is indication of the formation of clusters. Similar increase of low q has been observed in some liquids when they go from liquid to the spinodal region. These liquids after reaching the spinodal region change phase and form clusters or gels.[16] With larger formations of clusters, there does not need to be as high of an intensity of light required for the particles to reflect and scatter the light. Because it has been detected that there is a higher intensity of light scattered, this indicates that the higher velocities (v = 5,7 μm*s^{-1}) have a higher chance to form larger clusters as opposed to lower velocity systems.

From VMD, we can observe the formation of this cluster. Figure 3.3.4 shows the behavior of dynamic Brownian particles with a density of 0.3 that move at a rate of 3 μm*s^{-1}. With these systematic characteristics, the particles are forming into small clusters which can be seen in comparison to Figures 3.2.4 and 3.2.5. Any large cluster that forms will eventually split apart into two smaller clusters due to the particles' projection angling away from each other and not having enough particles in a certain time frame to interact with the cluster to allow for the cluster not to split.

Figure 3.3.4 ρ = 0.3 Velocity 3 μm*s^{-1}

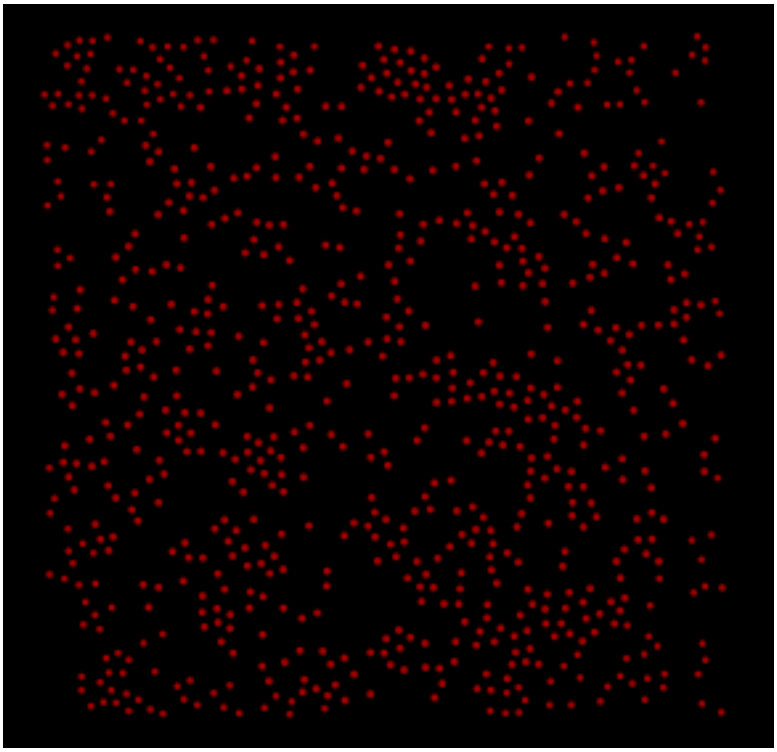

Figure 3.3.5 shows a dynamic system of Brownian particles with the same density of 0.3 as Figure 3.3.4, but it has a higher velocity of 7 μm*s^{-1}. It is seen in this figure that the clusters formed are larger in comparison to the clusters in Figure 3.3.4. This is due to the higher rate of particles interacting with each other not allowing for particles to leave a cluster or for the cluster to split into two or three smaller clusters.

Figure 3.3.5 ρ = 0.3 Velocity 7 μm*s^{-1}

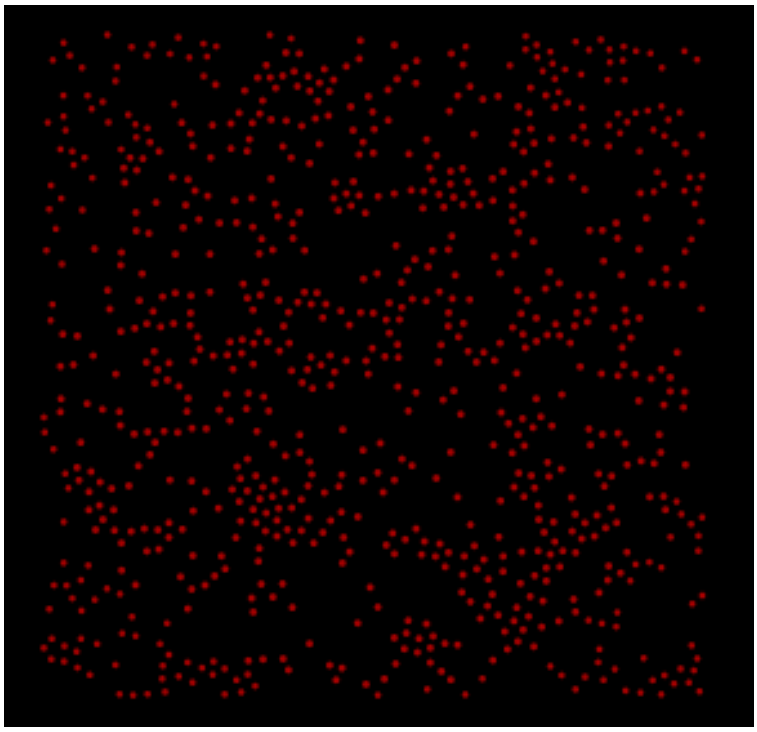

3.4 Thermodynamics

Previous research has looked into how various parameters such as temperature and microsphere diameter affect the viscosity of a system.[15] The experimental research that was just performed looked into changes in viscosity based on varying degrees of density for passive Brownian particles. Efforts are still being made to study viscosity for active Brownian particles with varying degrees in velocity. The simulation studies analyzed both passive and active Brownian particles.

Figure 3.4.1 shows the pressure changes of a system in which the particles are purely diffusive with a velocity of 0 μm*s^{-1}.

Figure 3.4.1 Pressure at varying densities with static collective motion

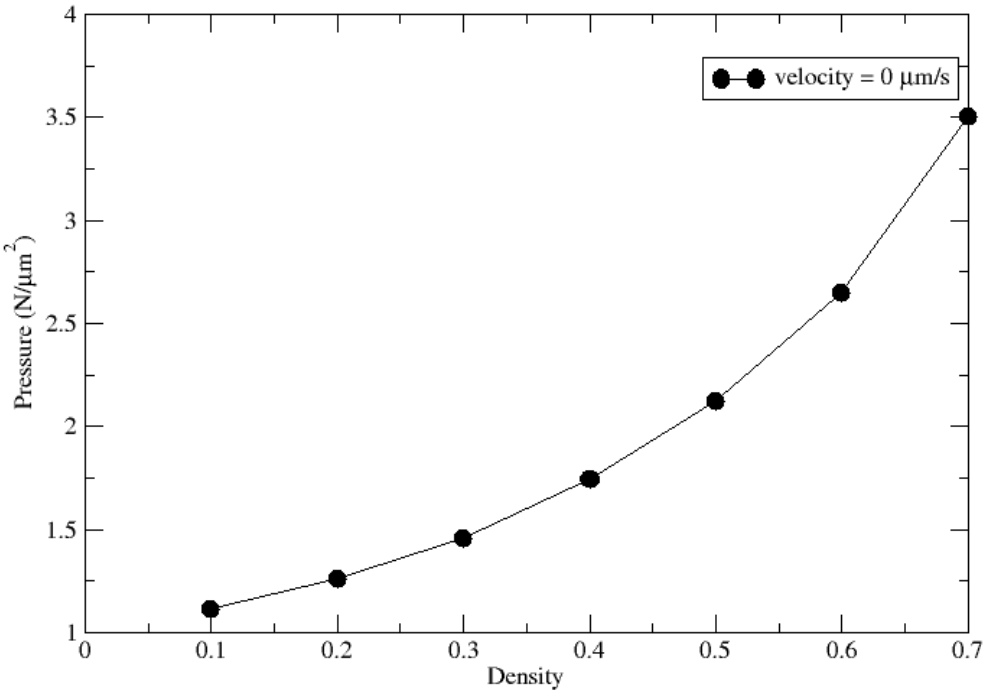

It can be seen that the pressure not only increases as the density increases, but it displays an exponential increase in pressure. This is not surprising given that the space in-between the particles is dramatically decreasing as the box size decreases. The particles have a higher likelihood of interacting with each other in higher density systems resulting in the increased pressure. With an exponential increase in pressure rather than a simple linear increase, it can be determined that pressure is strongly dependent upon the density of a system due to the interactions of the particles.

With the definition of an ideal gas that states the particles in an ideal gas do not interact with each other at all, this graph can be used to identify if a system falls under the ideal gas characteristics. The pressure would be determined to have 0 $\frac{N}{\mu m^2}$ because the particles should not be colliding into each other to result in a pressure being detected.

Figure 3.4.2 shows the change in pressure as the velocity increases. The density is constant at $\rho = 0.3$.

Figure 3.4.2 Pressure at varying velocities with $\rho = 0.3$

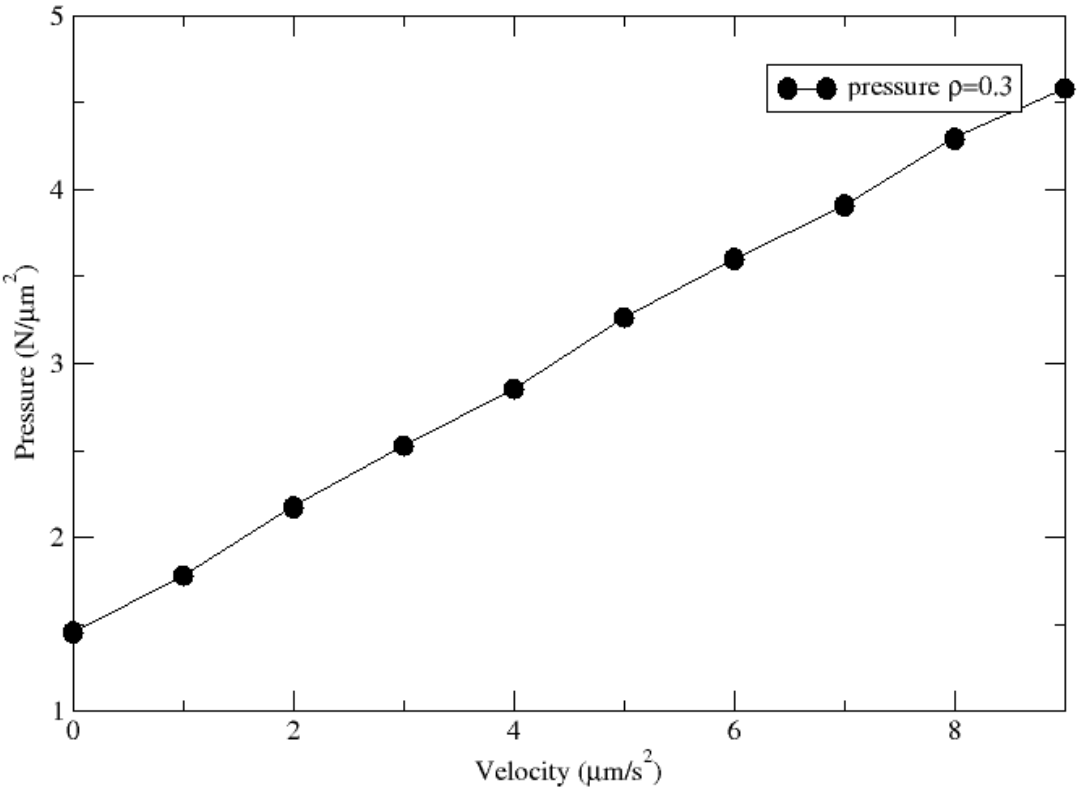

The change in pressure is kept at a constant increase as velocity increases. A higher velocity primarily just causes the particles to interact with each other easier but not more. If there is still plenty of space to allow particles to move around more, the particles will just simply move around at a faster rate. The linear increase determines that an increasing velocity does result in an increase in pressure, but pressure is not strongly dependent upon velocity as it is strongly dependent upon density, as seen in Figure 3.4.1.

Figure 3.4.3 demonstrates the trend in behavior of Brownian particles displaying diffusive passive behavior. The viscosity of passive particles has a higher affinity of shear thickening as the density increases in a static collective motion system.

Figure 3.4.3 Viscosity changes for v = 0 μm*s^{-1} as a function of ρ

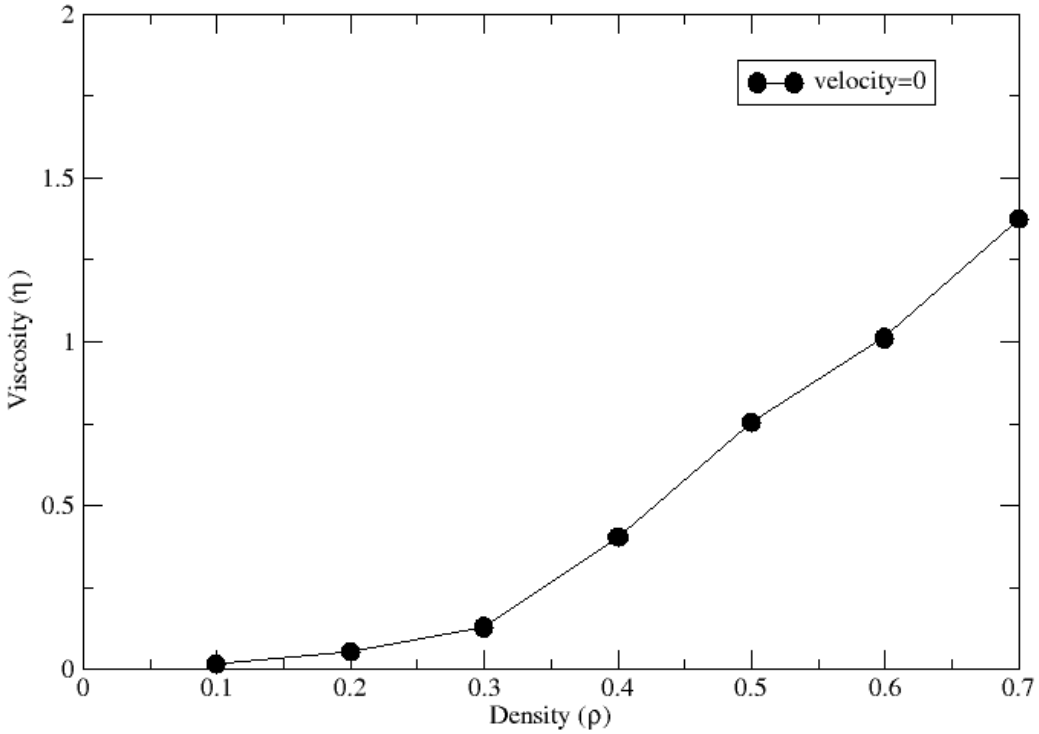

The explanation for the dramatic increase in viscosity once density hits 0.4 is that the clusters begin to split apart, but then those clusters increase in size through time resulting in a phase separation.

Figure 3.4.4 shows the trend of viscosity as velocity increases for a system with 0.3 density. The overall trend can be applied to any density of a system. It appears that the system goes under shear thickening as velocity increases. However, at 3 μm*s^{-1} and 7 μm*s^{-1}, the system experiences a sudden shift to shear thinning.

Figure 3.4.4 Viscosity as a function of velocity with $\rho = 0.3$

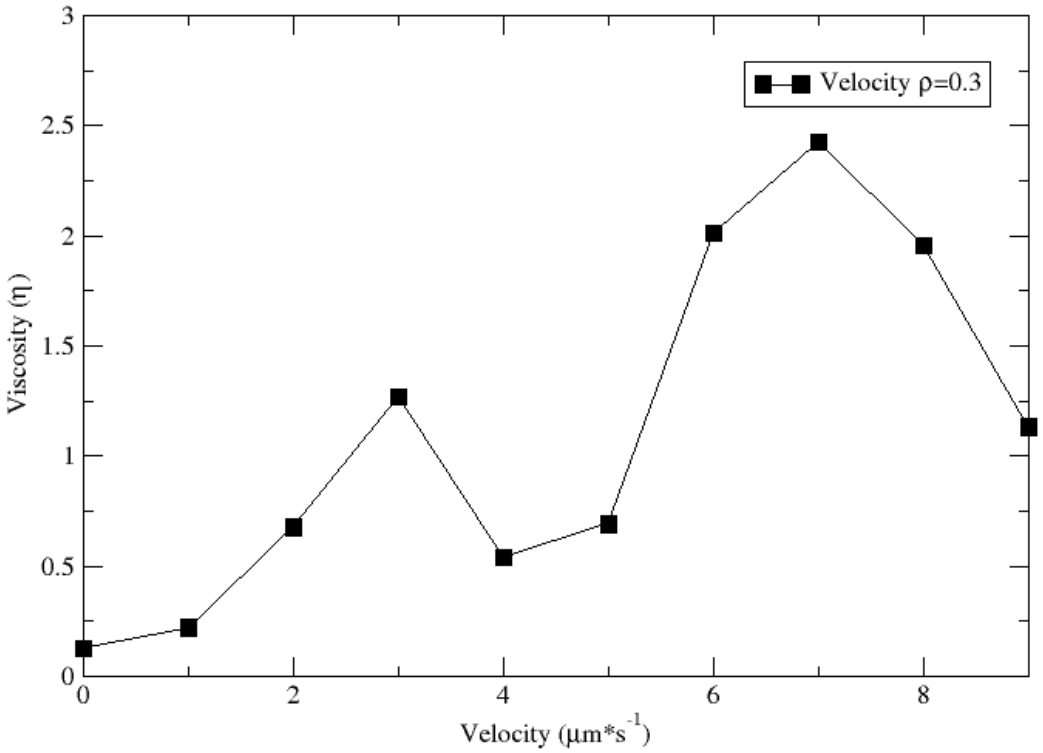

The explanation for the two velocities in which the system experiences shear thinning is that at 3 μm*s^{-1}, a large cluster just split into two smaller clusters. As velocity increases, the two smaller clusters begin to increase in size resulting in two large dynamic clusters interacting with each other. This leads to a phase separation of a few highly dense clusters surrounded by a dilute gas phase.

Figure 3.4.5 shows the experimental data for the varying degrees of density that was analyzed. The density is based on 1 drop or 2 drops per 100 mL of dH_2O. It is seen that the MSD remains unchanged based on the concentration. These particles exhibited passive Brownian behavior for 2.5 seconds. The trend line for the computational simulation is shown as a comparison of the MSD for a system with one particle with a velocity of 0 $\mu m*s^{-1}$.

Figure 3.4.5 Mean Squared Displacement for varying densities as a function of time

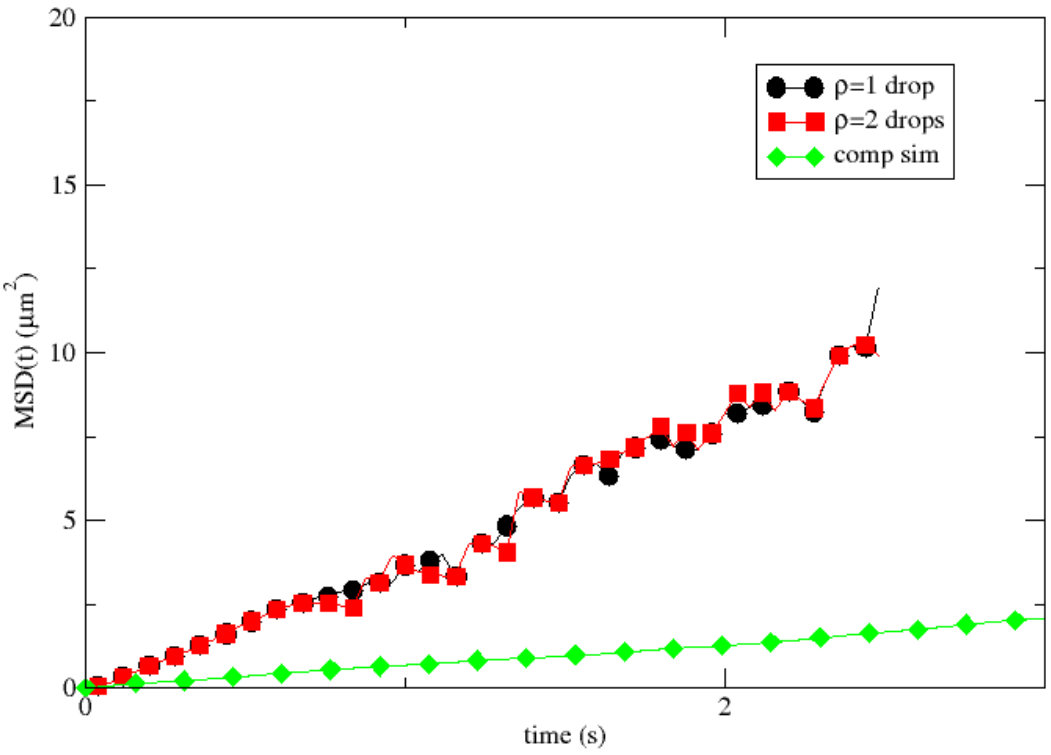

When visually observing the difference in density through the microscope, it was noticed that the concentration did not seem to have increased even though it doubled. When the coverslip was applied to the suspension on the microscope slide, it caused the sample to spread resulting in a higher concentration of particles to gather at the ridge of the concave portion of the slide. With this occurrence, it resulted in the particles to interact similarly towards the center of the sample even though the given concentration is different.

Figure 3.4.6 shows a group of particles interacting with each other. Because the velocity is held at 0 μm*s^{-1}, the viscosity is low which means that particles are not clustering together. This group of particles had a video taken, and the MSD was determined to form Figure 3.4.5.

Figure 3.4.6 Experimental image of polymer microspheres in static collective motion

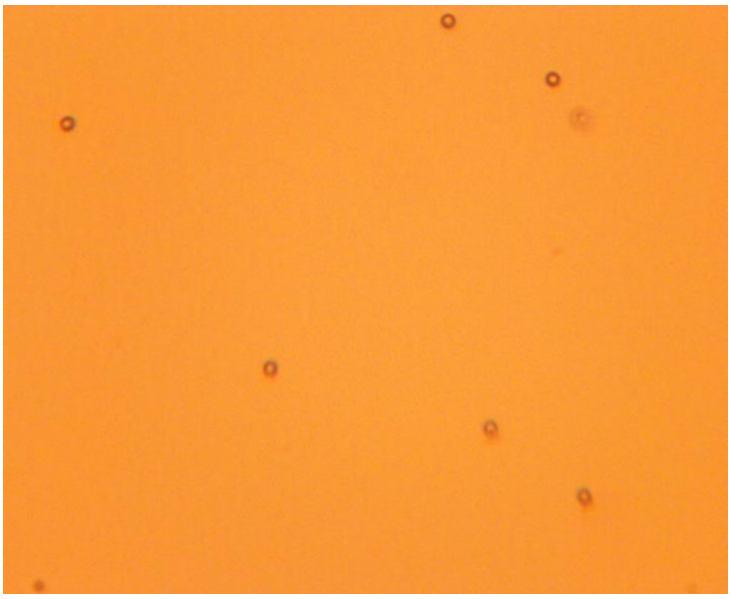

In the computational simulations, different forces such as attractive forces were able to be controlled and eliminated to determine how repulsive forces affect the behavior of the collective motion in a particle. However, the experiments that are described in Figures 3.4.5 and 3.4.6 involve the collective motion of polymer microspheres in which the attractive (hydrodynamic) forces are at a minimum due to the material makeup, but the forces are not completely eliminated. The affect that the hydrodynamic forces causes can cause a rippling effect similar to a boat in water. The after-shock wave caused by a boat to another object in the water can cause a bobbing motion which is experience and cannot be controlled in the experiments.

Figure 3.4.7 is an image of a single microsphere, and the video was analyzed to determine the MSD.

Figure 3.4.7 Experimental image of static, singular polymer microsphere

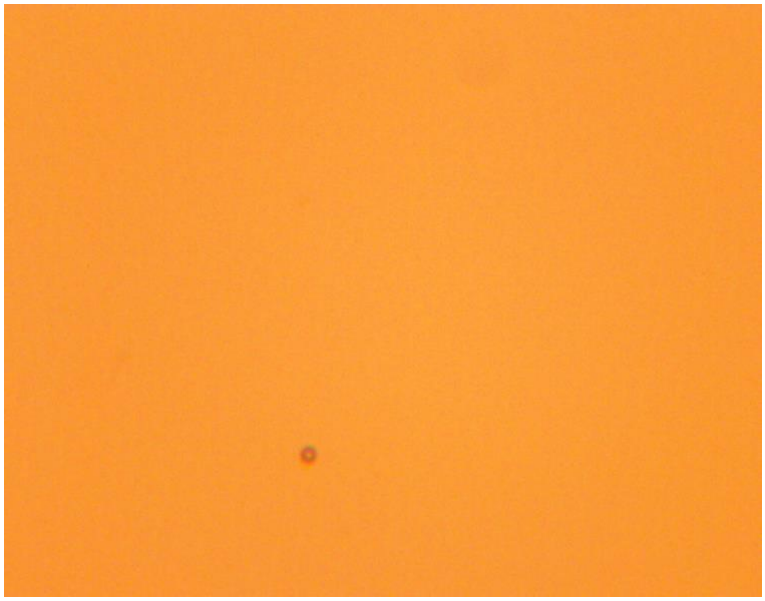

With the particle experiencing static behavior, and there are no other particles around to impose their interactive forces, the particle is purely moving through the deionized water with just diffusive motion. There is no chance of interaction with other particles which means the pressure of the system is at a minimum, and the viscosity remains essentially unchanged.

Conclusion

The purpose of this research is to expand upon the research that was previously done over soft-sphere particles and to explain the behavior pattern of the particles in static, dynamic, and complex fluid conditions. Interaction forces affect the behavior of particles which the differences can be observed in the singular particle and the collective motion experiments.[6] With the g(r) graph, Figure 3.3.2, showing that particles are still forming clusters even though the MSD graph, Figure 3.3.1, shows that the particles are moving a considerable amount of distance through time, this can be explained that the clusters as a whole are moving through space. The particles within each cluster are able to transfer from one cluster to another if their projection and surrounding particles allow such actions to proceed. The static graphs support this theory as well because the MSD graph, Figure 3.2.1, demonstrates that the largest densities travel the least amount thus allowing these systems to not move as easily as low-density systems. The g(r) graph, Figure 3.2.2, shows cluster formation for the high-density systems. The statics graphs support the dynamic clusters theory based on the formation and characteristics of the clusters based on varying degrees of density.

It is seen that, as an overall trend, viscosity increases as density and velocity increases. The increase in velocity can cause a short-term favorability towards shear thinning as clusters split apart, but then the viscosity increases as expected once those clusters increase in size. For static systems, the particles interact with each other the same amount for both densities as seen in Figure 3.4.5.

References

1. Volpe, G.; Gigan, S., Simulation of the active Brownian motion of a microswimmer. *Am. J. Phys.* **2014,** *82* (7), 659-663. DOI: 10.1119/1.4870398

2. Bechinger, C.; Leonardo, R. D.; Löwen, H.; Reichhardt, C.; Volpe, G.; Volpe, G., Active Particles in Complex and Crowded Environments. *Rev. Mod. Phys.* **2016,** *88*, 1-40.

3. Zöttl, A.; Stark, H., Emergent Behavior in Active Colloids. *J. Phys.: Condensed Matter* **2016,** *28*, 1-23. DOI:10.1088/0953-8984/28/25/253001

4. Ebbens, S. J., Active colloids: Progress and challenges towards realising autonomous applications. *Current Opinion in Colloid & Interface Science* **2015,** *10*. DOI: 10.1016/j.cocis.2015.10.003

5. Patteson, A. E.; Gopinath, A.; Arratia, P. E., Active Colloids in Complex Fluids. *J.COCIS* **2016,** *1*, 86-96. DOI: 10.1016/j.cocis.2016.01.001

6. Wagner, N.; Brady, J., Shear thickening in colloidal dispersions. *Physics Today* **2009,** *62* (10), 27-32.

7. Verberg, R.; Schepper, I.; Cohen, E., Viscosity and diffusion of concentrated hard-sphere-like colloidal suspensions. In *Dynamics: Models and kinetic methods for non-equilibrium many body systems*, Karkheck, J., Ed. NATO Science Series: Leiden, 1998; p 46.

8. Bechinger, C.; Leonardo, R. D.; Lowen, H.; Reichhardt, C.; Volpe, G.; Volpe, G., Active Particles in Complex and Crowded Environments. *Rev. Mod. Phys.* **2016,** *88*, 1-40.

9. Buttinoni, I.; al., e., Dynamical Clustering and Phase Separation in Suspensions of Self - propelled Colloid Particles. *PRL* **2013,** *110* (1103), 5. DOI: 10.1103/PhysRevLett.110.238301

10. Ermark, D. L.; McCammon, J. A., Brownian dynamics with hydrodynamic interactions. *J. Chem. Phys.* **1978,** *69* (4), 1352.

11. Humphrey, W.; Dalke, A.; Schulten, K.; Stone, J. *Visual Molecular Dynamics*, University of Illinois at Urbana-Champaign: 2016.

12. Allen, M. P.; Tildesley, D. J., *Computer Simulations of Liquids*. Oxford University Press: New York, 1987.

13. Allen, M. P.; Tildesley, D. J., *Computer Simulation of Liquids*. Oxford University Press: New York, 1987.

14. Allen, M. P.; Tildesley, D. J., *Computer Simulations of Liquids*. Oxford University Press: New York, 1987; p 60.

15. Jia, D.; Hamilton, J.; Zaman, L.; Goonewardene, A., The time, size, viscosity and temperature dependence of the Brownian motion of polystyrene microspheres. *Am. J. Phys.* **2006,** *75* (2), 111-115. DOI: 10.1119/1.2386163

16. Sanz, E.; Leunissen, M.; Fortini, A.; Blaaderen, A.; D'ijkstra, M., Gel formations in suspensions of oppositely charged colloids: Mechanism and relation to the equilibrium phase diagram. *J. Phys. Chem. B.* **2008,** *112* (35), 10861-72. DOI: 10.1021/jp801440v